FAILURE ANALYSIS OF IMPELLER BLADE CRACKING IN A MECHANICAL VAPOUR RECOMPRESSOR (MVR) FAN

Brian DONOHUE, Milo KRAL

Department of Mechanical Engineering, University of Canterbury, New Zealand

SUMMARY

A root cause failure analysis was carried out following blade loss in a fan that had 150 hours of operation following commissioning. The cause was linked to harmonics in the VSD motor control that excited the second torsional mode of the rotating assembly. Once corrected the fan ran for two years before further cracking was observed during routine maintenance. The new cracks were generated by a different mechanism and further analysis revealed a coupled bending and rotation mode problem that had been masked by the magnitude of the initial second torsion mode motion during the first investigation.

INTRODUCTION

Three milk powder production facilities were recently commissioned in New Zealand, the plants are essentially identical. One plant processes fifty percent more milk volume that the others but all have the same potential total capacity. The production system involves an evaporation process to remove water from milk to produce powder. The fan used to circulate powder through the drier is a mechanical vapour recompression fan, shortened to MVR. Shortly after commissioning of the higher production factory, the MVR fan suffered a catastrophic loss of a blade. Travelling at 730km/h, the blade travelled up the discharge duct and into the evaporator destroying many tubes along the way. The plant was only 150 hours old. Needless to say there was a high level of concern, not only on safety grounds, but because of the risk of failure in the other plants and there were also several similar fans installed in plants around the world. A brief examination of the fracture surfaces of the broken blade revealed that fatigue had occurred close to both welded edges where it connected with the front-ring and backplate of the impeller. Scanning electron microscopy confirmed that this was the case. Figure 1 shows the impeller and the area where the blade was ejected.

This was a complex failure with many candidate causes and there was considerable pressure to remedy the problem and get the plant back in to production. Another failure occurred a few years later. The crack surfaces of the failed blades again showed fatigue, but this time from a different cause. The first failure was reported [1] but some recommendations have not yet been adopted.

Figure 1 Photograph of the MVR impeller with missing blade

BACKGROUND

The MVR fan is only one component in a complex industrial process. There is a lack of redundancy so a catastrophic failure is not only expensive in terms of repair or replacement cost, but also in lost production. A shut down can mean that milk must be processed elsewhere or run to waste. The MVR fan system consists of an induction motor driving a MVR fan through a coupling as shown in Figure 2. The motor speed is controlled by a variable speed drive (VSD) configured to change the fan speed according to evaporator loading. The fan impeller weighs around 1400 kg, has 16 full length blades and 16 short blades and operates over the speed range from 300 rpm to 2115 rpm. Once production starts the fan runs continuously.

Figure 2: The MVR fan

The impeller was entirely fabricated from duplex stainless steel plates by TIG and MIG welding – a normal requirement for sanitary applications such as dairy. The overall impeller diameter is approximately 2 metres with an inlet diameter of approximately 750 mm and hub height of approximately 500 mm. The front ring of the impeller varies in thickness from 10mm to 25mm in 2205 duplex, the backplate is fabricated from 8mm and 12mm duplex, and the blades from 6mm LDX 2101 duplex. There are 32 blades in total, one set that are full length and span from the inlet ring to the discharge, and a shorter set that are spaced intermediate to the long blades. The weld filler material was 2205. The impeller was dynamically balanced in the factory prior to dispatch and field balanced in-situ during commissioning. In the first failure event where a blade was thrown (mass around 3kg), a considerable unbalance was generated sufficient to shake the whole building. The impeller was rotating at 1950rpm at the time the failure occurred.

VISUAL EXAMINATION

At the outset the study concentrated on material failure, as the first thoughts were of possible weld defects, laps, heat affected zone, residual stress, and other issues associated with weldments. Visual inspection had shown a possible lack of fusion as the failed blade had simply pulled out of the weld with little adherence evident. Dye penetrant testing revealed crack indications on almost every blade weld. The presence of residual tensile stresses was indicated by yawning cracks at blade edges, see Figure 3. A cracked blade was cut away from the impeller and the crack opened up for examination. Beach marks were visual indications of fatigue and numerous initiation sites could be seen on either side of the blade. Scanning electron microscopy revealed the presence of fatigue striations which was clear evidence that fatigue was the cracking mechanism; see Figure 4 (from [1]).

Figure 3: Photographs showing typical cracks evident at several short blade location, showing residual tensile stress

(a)  (b)

Figure 4 (a) Opened cracks showed the classic visual appearance of fatigue with many initiation sites on either side of the blade as indicated by arrows and (b) Scanning electron microscopy showed fatigue striations on the thrown mid-blade fracture surface.

At this point in the analysis, it was only clear that fatigue was the fracture mechanism and that there was a lack of fusion in the thrown blade. However, other fan blades were cracked as well. One possible explanation for the impeller failure was that the blade with a defective weld had fatigued due to resonance then severe vibrations occurred due to imbalance after the blade was thrown, which in turn resulted in other cracks being formed. So, a root cause analysis [2] was carried out since a source of stress to drive fatigue crack growth in the thrown blade had not been immediately identified. In seeking a source of stress, two vibration modes were conceptually identified: a blade 'flapping' mode and a torsional mode - see Figure 5.

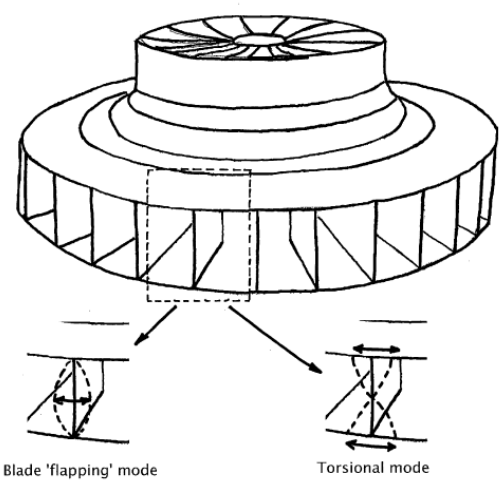

Figure 5: Two possible modes of blade vibration

Thus, the first step was to calculate and measure the natural frequencies for structural modes of vibration of the blades, and the torsional frequency for the impeller (front ring relative to back plate). In addition, an impulse response procedure was used to confirm the calculated values. Initial calculations indicated the three lowest blade ''flapping" modes were 438 Hz, 567 Hz and 1037 Hz. These compared well with the measured modes of 422 Hz, 586 Hz and 1055 Hz respectively. An impact response test using an accelerometer gave an indicated torsion response at 94 Hz. This was for the impeller only, lying on the ground – as in Figure 1, without the shaft coupling and motor armature. However, the test indicated that there was a modal frequency that could be excited by variations in torque related to line frequency (i.e. 50 Hz and 100Hz).

Simplified models were then developed using measurements taken from the failed impeller, see Figures 6 and 7, in order to gain a better insight into the resonant motion.

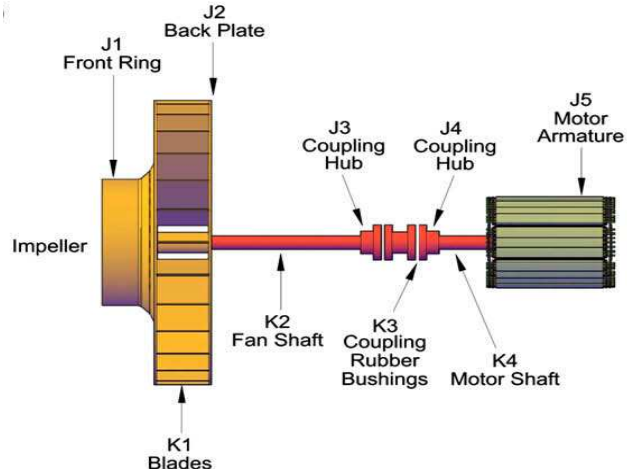

Figure 6: Model for torsional analysis

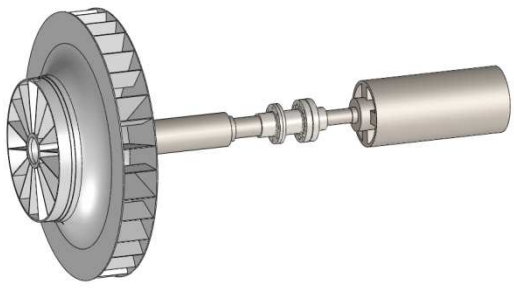

Figure 7: Model of the MVR rotating assembly for FEA

TORSIONAL ANALYSIS

Data could not be obtained from the fan manufacturer and considerable time was spent in locating information that was required for the analysis - from the coupling and motor suppliers as well as in the measuring and modelling of the impeller. The stiffness of the blades was estimated from bending theory, where those for the fan and motor shafts were readily calculated. The coupling was problematic in that coned elastomeric inserts were used who's stiffness varies with applied torque. In our initial calculations the stiffness was assumed to be linear, taking an averaged catalogue value. At this stage the objective was to determine whether in fact there could be a modal frequency with a low enough value as to be excited by mechanical or electrical sources. Time had not permitted construction of the solid model at this stage as there was urgency to return to production.

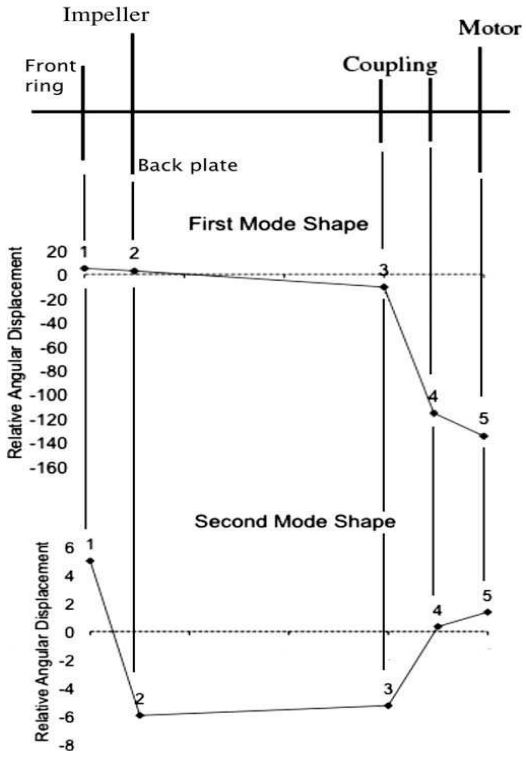

Figure 8: Mode shapes for vibration in torsion

The mode shapes (Figure 8) obtained from the analysis showed that for the first mode the nodal point is situated approximately at the in-board fan bearing. In the second mode there are nodal points between the impeller backplate and frontring and at the coupling, showing that the second mode vibration has reversed torsional loading at the impeller and coupling. The mode shapes did not vary much when adjusting the coupling stiffness in the analysis to allow for non-linearity. However, the first modal frequency increased from 8 Hz to 33 Hz. The analysis showed that the first mode was always within the speed range of operation, 300 rpm (5 Hz) to 2150 rpm (35.83 Hz), where at 72 Hz the second mode was outside the operating speed range. FEA studies confirmed that there was a variable frequency first torsion mode due to non-linear coupling stiffness and that the second mode frequency remained unchanged. The FEA study was based on the solid model shown in Figure 7. The model was a simplified version of the actual impeller, where the blade form is not exact as details were not available to enable proper modeling.

The first mode is likely to always be excited, where the second mode requires a harmonic for excitation. Continuous excitation occurs because the system is lightly damped and there are torsional variations in load from the process and variations in speed from the VSD controller. Subsequent strain gauge tests, using telemetry equipment on the fan shafts at other plants, showed that there were variations in torque of the order of ± 15% - which apparently are within the limit allowable for the coupling.

So, analyses had shown that there was a possible response of impeller blades in a flapping mode excited by aerodynamic or fluid loading sources from CIP for example, together with the possibility of two torsional modes being excited by variations in torque inherent in the production process.

For each torsional mode, node crossings (amplitude equal to zero – see Figure 8) usually indicate areas with highest stress while antinodes (high amplitude) indicate maximum angular oscillation. Based on the calculated mode shapes shown in Figure 8, the first torsional natural frequency would be responsible for causing fatigue cracks in the shaft keyways near the coupling hubs and damaging the coupling rubber elements. The 2nd mode is the one most likely to cause a large oscillatory motion between the impeller front and back plates. The damaging effect of 2nd mode oscillations is

by rotating the impeller frontring and backplate in opposite directions (twisting), which in turn causes large strains at the blade welds as a result of the reversed bend displacement of the blades as shown in Figure 9(b).

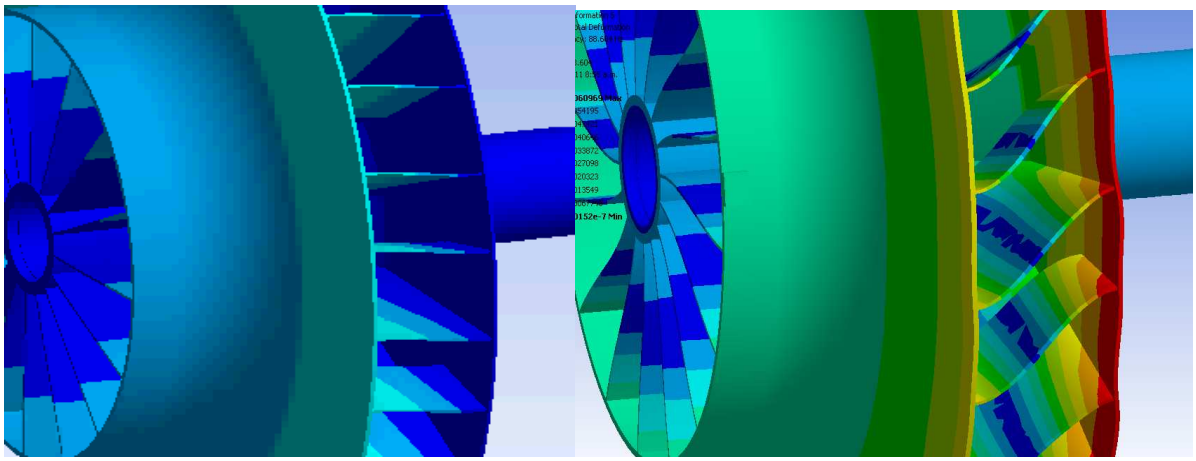

(a) (b)

Figure 9: Modal displacements of blades in torsion – from an FEA study (a)in first mode (b) in second mode

A Campbell or interference diagram (Figure 10) is very useful for illustrating the areas of torsional vibration risk in a rotating assembly. The Campbell diagram is obtained by plotting the torsional natural frequencies against the frequencies of possible sources of excitation - the shaft speed (open squares) and controller frequency (filled triangles). Note that couplings with elastomeric elements introduce more uncertainty into the torsional calculations and can have torsional stiffness values that are ± 25% from published catalogue values.

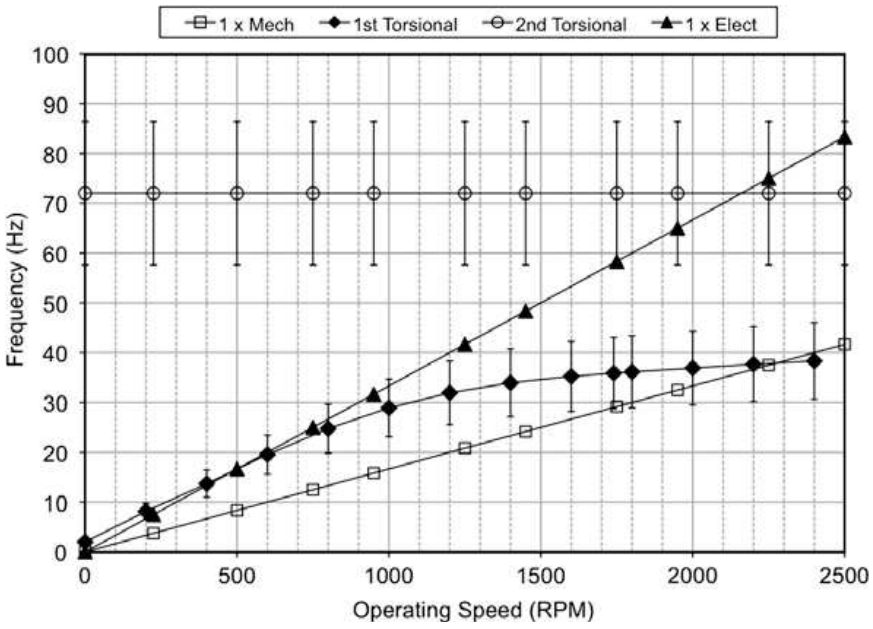

Figure 10: Interference diagram (Campbell)

There are several issues highlighted by the Campbell diagram:

- It can be seen that there is a close correspondence between the 1x Electric line (triangles) and the 1st torsional mode line (diamonds) from 0 rpm up to about 800 rpm, suggesting that this would

deliver pulses from the VSD at a frequency that virtually corresponds to the first torsion mode natural frequency. This will excite the 1st mode and potentially drive the system unstable.

- From 1750 rpm upwards, the 1st torsion modal frequency ±20% (indicating the region for design where natural frequencies should be avoided) overlaps with the 1x mechanical (i.e., shaft speed) and is at risk of being excited by the shaft rotation alone. This has nothing to do with the VSD controller, but is to do with a low coupling stiffness (a higher coupling stiffness would lift the first mode torsional line clear of the 1x mechanical line).
- The 1x Electric frequency line (triangles) overlaps with the 2nd torsional mode frequency line from about 1800 rpm onwards. This means that the VSD controller will deliver pulses at a frequency that correspond to, and excite the 2nd mode directly. The centre of this range is very close to 2150 rpm, the maximum running speed for the impeller.
- The VSD generates a side frequency (equal to 100 Hz minus the set point frequency) and this also can cause excitation of the torsion modes.

The solution to the problem of rapid fatigue failure was to use a V/Hz motor controller (open loop), rather than the SVC controller algorithm (with 'virtual feedback') that was in use. This avoided significant excitation from the controller and was adequate for the MVR process. Following a change to the V/Hz control, a waterfall plot of the fan shaft torque showed that there was little excitation of the second torsion mode– see Figure 11. However, the 1st mode torsion remained but pressure to return to production precluded a study to determine its severity.

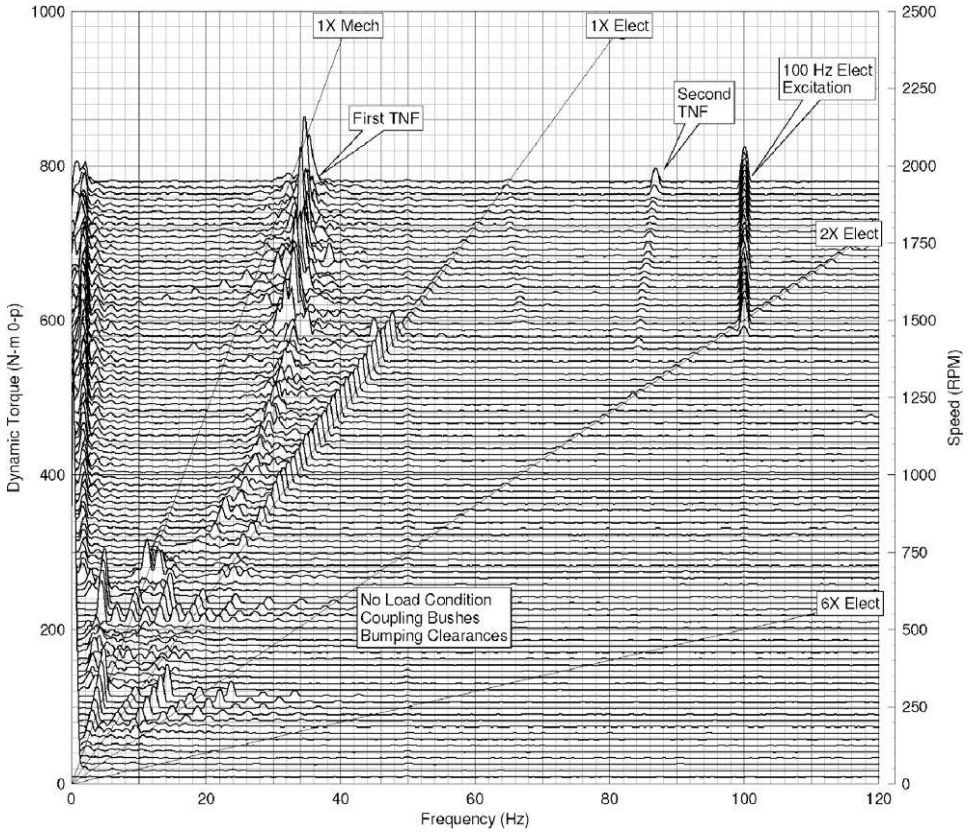

Figure 11: Waterfall plot taken form torque measurement data during a shut down [1]

FORWARD TO 2010

Eighteen months of operation later and further cracking was noticed during a routine annual maintenance inspection. The cracking was not considered to be significant enough to warrant a shut down and so the plant was returned to operation until the next maintenance inspection, when the

current investigation began. Dye penetrant now revealed extensive cracking but this time only on the pressure side of the blades (Figure 12). Only short blades were cracked and these exhibited an unusual pattern. The cracks appeared at the toe of welds on the front ring edge and were relatively long – around 120 mm. The cracks at the backplate edge of the blades were short – around 30 mm, in parent material and orientated along a blade diagonal – see Figure 13. One blade contained a crack that had propagated through the whole thickness (5 in Figure 13). Scanning electron microscopy (Figure 14) showed that failure was due to low cycle high load fatigue with perhaps 5 to 10 thousand cycles. As cracking had occurred during the previous 2 years of operation, the loading events required could be represented by single isolated events of severe loading, a random or isolated packet of cyclic loading, or repeated periodic low cycle events. Figure 13 shows there were more long cracks than short cracks and that they appeared to be distributed about a diametral line.

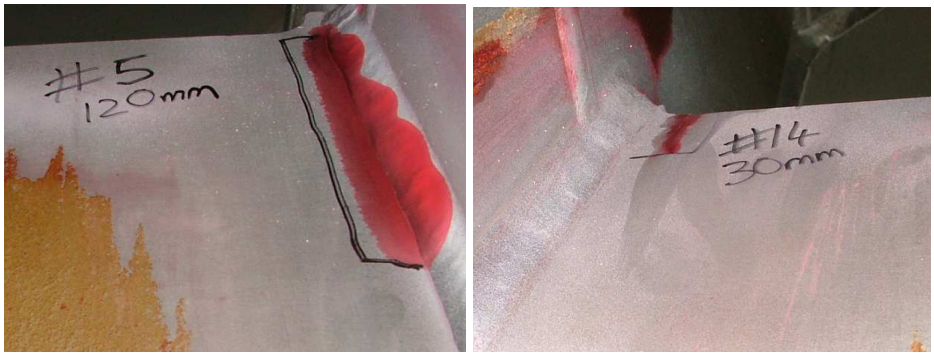

(a) **(b)**

Figure 12: Dye penetrant on blades showing (a) long crack and (b) short crack types

Torsional vibration was eliminated as the cause in this second failure as the cracking was on some blades only and from one side of the blades only, where in the first case all blades were cracked and exhibited on both sides of the blades.

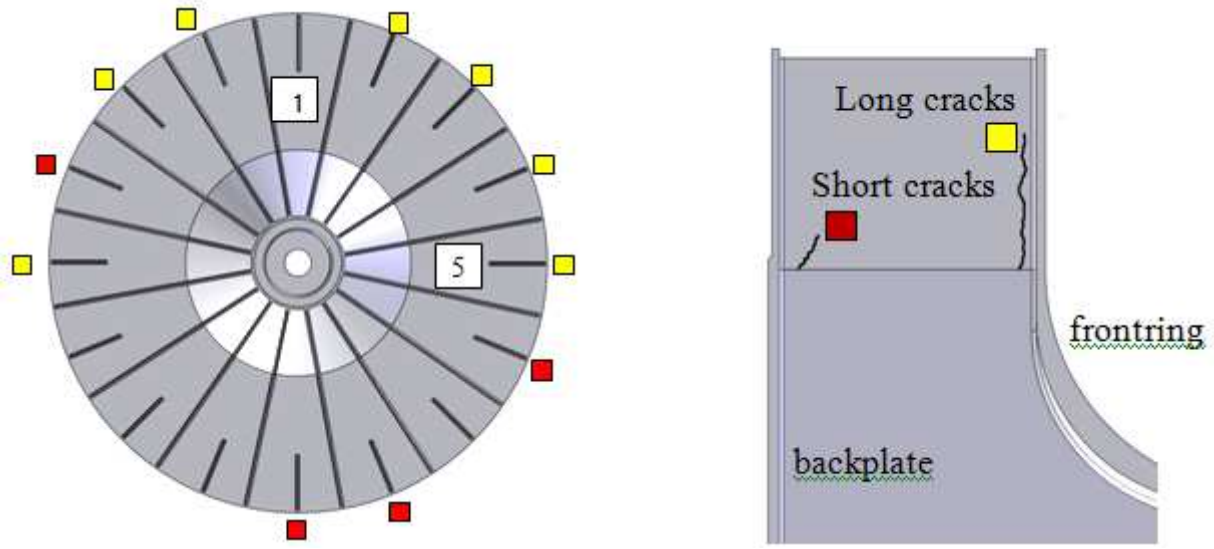

Figure 13: Sections through the impeller showing locations of the two types of crack
Note: only the short blades were cracked

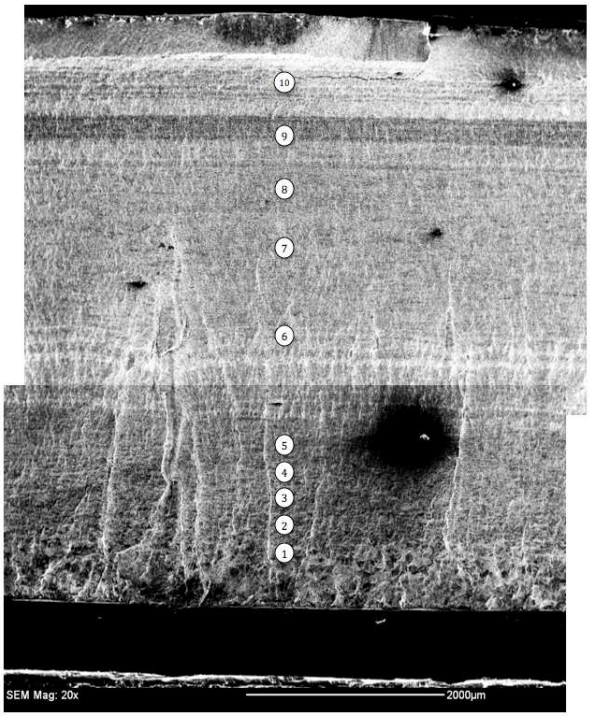

Figure 14: Montage of scanning electron images from the crack surface of a blade with a through crack. The numbered white circles indicate locations at which higher magnification images were taken for striation spacing measurements.

A list of possible exciting forces and events was drawn up and a root cause analysis (RCA) tree constructed along with a decision table that ranked each event for likelihood of being a major contributor. In support, by way of generating the factual data (necessary for RCA), a run-up speed test was conducted whilst monitoring shaft strain and bearing vibration. No unusual torque deviations were noted (except for a ground loop that saturated our strain data) but a resonance in the bearing vibration was noted at 1470 rpm – Figure 15. The red trace is the fan speed with a stepwise incremental region in 50rpm steps. The blue trace is the bearing vibration velocity.

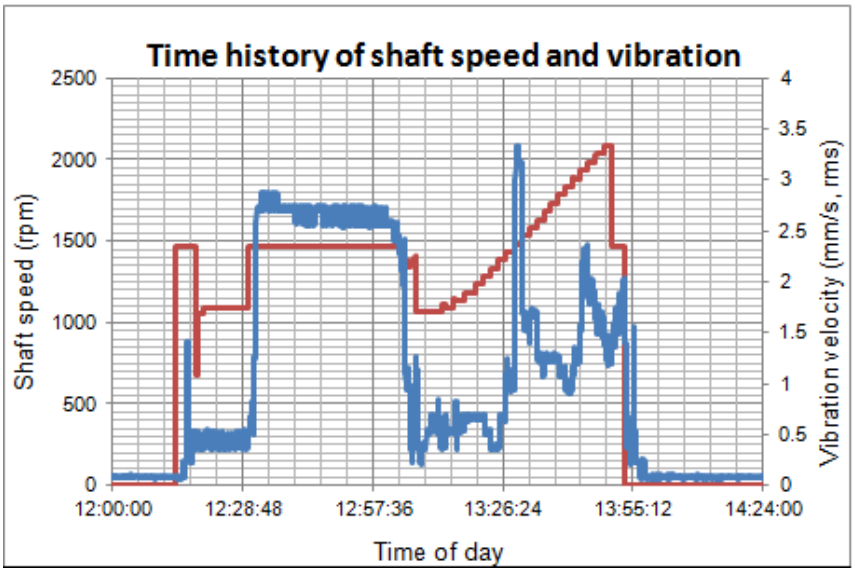

Figure 15: Plot for vibration response on run up speed tests shows resonance at 24.5Hz

The run up test was then followed by impact response testing of the impeller and shaft. This showed an asymmetric response of the shaft with bend modes at 41 Hz vertically and 35 Hz horizontally. The asymmetry was attributed to the in-board fan bearing - a rolling element roller

bearing with a diametral clearance of 200 microns. The gravity load keeps the shaft in contact with the rollers at the lowest point of the bearing; this provides a higher stiffness in the vertical plane than in the horizontal plane. It was suspected that the dynamic stiffness of the bearing would be lower than its static stiffness during the impact tests, so a series of analyses was carried out using FEA software to study the effect of varying the bearing support stiffness. This showed that the predicted bend mode can occur over a wide frequency range according to bearing stiffness – Figure 16.

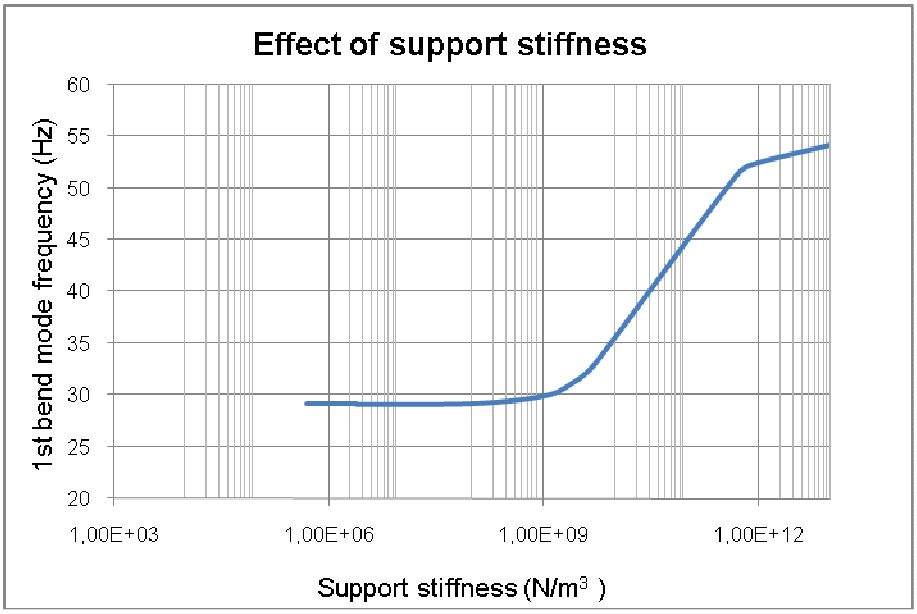

Figure 16: Plot of 1st bend mode frequency for the MVR rotating assembly

There then appeared to be a high probability that the measured 24.5 Hz resonance was a transverse bend mode in the horizontal plane where the stiffness has its lowest value. It would appear that excitation comes from imbalance (and possibly gyroscopic torque) that is caused by the rotor sitting lower than the axis of rotation by some 250 to 300 microns because of clearance in the bearing. Thus the bend mode is synchronous with rotation – a critical speed. That is, the shaft exhibits a whirling motion where the orbit is flattened in the vertical plane due to the gravity load and horizontal motion is limited by the clearance in the bearing. Vibration occurs only when the fan is running at, or passing through, this critical speed of 24.5 Hz (1470 rpm). Unfortunately, at this time, there was no possible way to install proximity sensors to monitor shaft motion and the bearing housing cover will have to be modified to allow access for probes. Testing to determine shaft displacement and blade strains during processing are planned for the next annual maintenance shutdown.

Observation of the plant's PLC (programmable logic controller) screen records showed a daily event where the critical speed is passed through twice each day. The event occurs for CIP (clean in place) when the fan slows down, is cleaned and then runs up to normal operating speed. Figure 17 shows a typical PLC screen for the MVR fan, where the black trace shows the fan shaft speed, the blue trace shows the vibration level, and the process step number (that shows CIP has been called) is shown by the green trace.

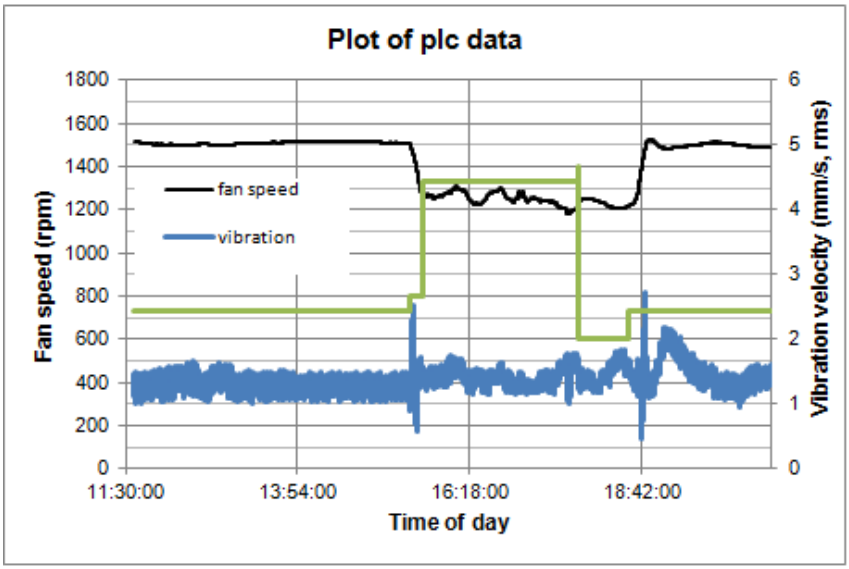

Figure 17: plc screen display showing correlation between vibration events and fan speed

.

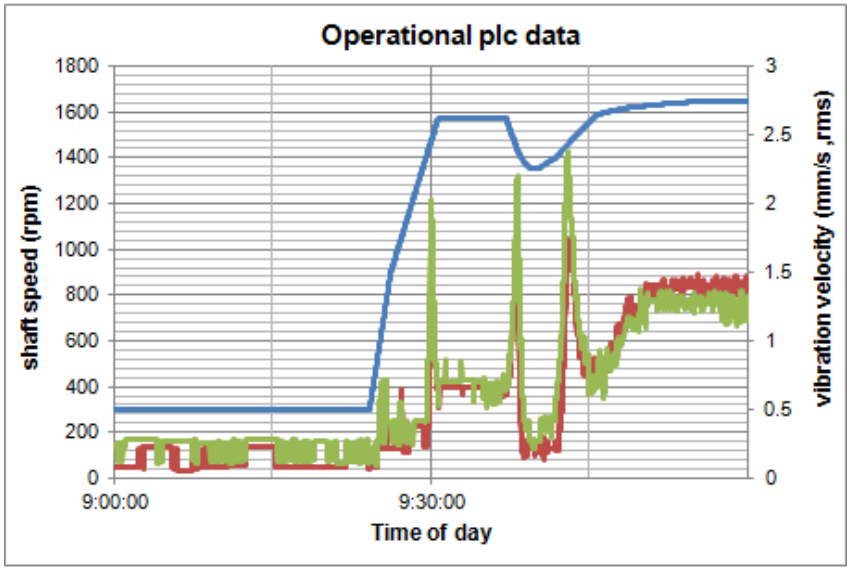

Figure 18: plc data for newly commissioned MVR fan

Tests at a more recently commissioned new factory showed the same correlation between vibration level and speed change – see Figure 18. The blue trace shows the fan speed where the green and red traces are the vibration levels taken at the in-board and out-board fan bearings respectively. Note that whilst the vibration levels appear to be low, the sensor monitors motion of the bearing housing (and pedestal) and not the motion of the impeller. It is possible for the impeller to have a much greater peak level of vibration that is not 'seen' by the relatively slow scanning speed of the plc logger.

The current hypothesis for the mechanism of failure is that the shaft undergoes a sharp whirl for perhaps three cycles as it passes through the critical speed on either ramp up or ramp down. The whirl is limited by the clearance in the roller bearing where the impeller deflection is limited by the restoring force in the shaft. One CIP event per day would equate to around 4000 cycles over two years operation, which is consistent with the forensic metallographic observations.

At the present time, the root cause analysis has converged on a shaft whirl due to bearing asymmetry as the mode of failure – yet to be confirmed by testing. The final root cause can only be determined by the manufacturer however since it apparently lies in the design process.

CONCLUSIONS

A large centrifugal type fan impeller has failed through metal fatigue on two occasions over a three year time period by two different mechanisms. The mechanism of the first failure was readily identified as torsion excited by oscillations generated by the motor control algorithm. This could only occur because there was a natural frequency of the rotating assembly in torsion that could be excited by drive frequencies in the fan's operating speed range. This was resolved by providing a simple change to a different control algorithm. However, this did not remove the first torsion mode of vibration, which is still of concern.

The mechanism of the second failure was not so readily identified and the current hypothesis needs to be confirmed by testing during the next shut down, assuming no earlier failure event occurs. In any event there is a lateral critical speed in the operating speed range at which a resonance is apparent but whose effect has yet to be evaluated.

REFERENCES

[1] Alexander, K., et al. *Failure analysis of an MVR (mechanical vapour rescompressor) impeller.* Eng. Failure Analysis **2010**.

[2] Mobley R.K., *Root cause failure analysis*. Oxford UK: Butterworth, **1999.**

[3] Nestorides E.J., ed. *A handbook on torsional vibration*. Cambridge UK: Cambridge University Press; **1958**.